

See discussions, stats, and author profiles for this publication at: <https://www.researchgate.net/publication/46182399>

# IR Spectroscopic Characterization of the Thermally Induced Isomerization in Carbon Disulfide Dimer Anions

ARTICLE *in* JOURNAL OF PHYSICAL CHEMISTRY LETTERS · AUGUST 2010

Impact Factor: 7.46 · DOI: 10.1021/jz100841e · Source: OAI

---

CITATIONS

4

---

READS

42

6 AUTHORS, INCLUDING:



**Andrei Sanov**

The University of Arizona

**103** PUBLICATIONS **1,452** CITATIONS

SEE PROFILE



**Knut R Asmis**

University of Leipzig

**103** PUBLICATIONS **2,473** CITATIONS

SEE PROFILE

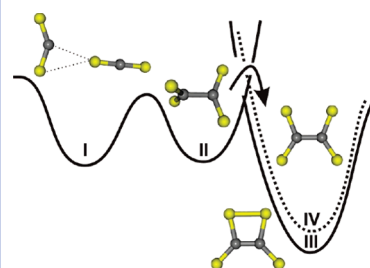
# IR Spectroscopic Characterization of the Thermally Induced Isomerization in Carbon Disulfide Dimer Anions

Daniel J. Goebbert,<sup>†</sup> Torsten Wende,<sup>‡</sup> Ling Jiang,<sup>‡</sup> Gerard Meijer,<sup>‡</sup> Andrei Sanov,<sup>\*,†</sup> and Knut R. Asmis<sup>\*,†</sup>

<sup>†</sup>Department of Chemistry and Biochemistry, University of Arizona, Tucson, Arizona 85721-0041, and <sup>‡</sup>Department of Molecular Physics, Fritz-Haber-Institut der Max-Planck-Gesellschaft, Berlin 14195, Germany

**ABSTRACT** We report experimental vibrational spectra of thermalized carbon disulfide dimer anions,  $(\text{CS}_2)_2^-$ , measured at ion trap temperatures from 16 to 300 K. Previous experiments showed evidence for several  $(\text{CS}_2)_2^-$  isomers, whose relative abundance depends on the source conditions. We used infrared (IR) photodissociation spectroscopy in the fingerprint region ( $550\text{--}1600\text{ cm}^{-1}$ ) of  $(\text{CS}_2)_2^-$  thermalized in a temperature-controllable ion trap, in combination with simulated IR spectra derived from ab initio calculations, to identify the isomers present at various ion trap temperatures. The IR photodissociation spectra show characteristic signatures for at least three different isomers. Anions formed in the source are primarily trapped as high-energy ion–molecule complexes, in which the unpaired electron is localized on a single  $\text{CS}_2$  moiety. Thermal heating supplies sufficient energy to overcome the isomerization barriers and shifts the isomer population via a weakly bound isomer, in which the electron is delocalized over the complete complex, to lower-energy covalently bound structures.

**SECTION** Kinetics, Spectroscopy



The carbon disulfide dimer anion represents a prototypical system to study the influence of solvation on electronic structure. The monomer unit  $\text{CS}_2$ , widely used in organic synthesis, is isovalent with  $\text{CO}_2$  but exhibits quite different properties, for example, a three times higher polarizability and a positive electron affinity.  $(\text{CS}_2)_n^-$  as well as  $(\text{CO}_2)_n^-$  clusters have served as fruitful model systems to study the size dependence of solvent-mediated structural deformation as well as charge delocalization processes.<sup>1–5</sup> Several experimental studies on the dimer anion,  $(\text{CS}_2)_2^-$ , have confirmed the presence of multiple isomers, whose relative abundance depends on the ion production conditions.<sup>3,4,6–10</sup> To characterize the structure and stability of the different isomeric forms of  $(\text{CS}_2)_2^-$ , we have measured temperature-dependent vibrational spectra of  $(\text{CS}_2)_2^-$  thermalized in a buffer gas filled, temperature-controllable ion trap. The results provide compelling spectroscopic evidence for the thermally induced conversion of the weakly bound ion–molecule complex,  $\text{CS}_2 \cdot \text{CS}_2^-$ , via an intermediate complex, to covalently bound  $\text{C}_2\text{S}_4^-$ .

The structure of  $(\text{CS}_2)_2^-$  has long been controversial. It is typically formed via electron attachment to neutral  $(\text{CS}_2)_n$  clusters in a supersonic expansion. Anion photoelectron spectra by Bowen and co-workers<sup>6</sup> revealed a weakly bound  $\text{CS}_2 \cdot \text{CS}_2^-$  complex with a solvation energy (with respect to  $\text{CS}_2^-$ ) of 0.18 eV, while equilibrium measurements<sup>10</sup> at elevated temperatures yielded evidence for a covalently bound species ( $D_0 = 0.95\text{ eV}$ ). Several later studies<sup>3,4,7–9</sup> confirmed the presence of multiple isomers. Photodissociation

showed formation of  $\text{S}_2^-$  and  $\text{C}_2\text{S}_2^-$  fragments, consistent with a covalently bound isomer which contains a four-membered ring with S–S and C–C covalent bonds.<sup>4,7</sup> Recent anion photoelectron spectra resolved a vibrational progression characteristic of a cyclic structure involving a  $C_{2v}$  isomer ( $^2B_1$  electronic state).<sup>9</sup> A second covalently bound isomer, with a 0.5 eV higher vertical detachment energy, has also been observed<sup>3</sup> and attributed<sup>9</sup> to the  $^2B_2$  state of  $\text{C}_2\text{S}_4^-$  with  $C_{2v}$  symmetry.<sup>8</sup> Recently, Kobayashi et al. investigated the IRPD spectra of  $(\text{CS}_2)_n^-$  clusters ( $n = 3\text{--}10$ ) in the region from 1100 to 2000  $\text{cm}^{-1}$ .<sup>5</sup> The spectra showed features characteristic of a  $\text{CS}_2^-$  ion core. The region below 1100  $\text{cm}^{-1}$ , probed in the present experiments, is expected to reveal fundamental modes of the covalently bound dimer anions.

Much uncertainty regarding the nature of the covalently bound  $\text{C}_2\text{S}_4^-$  structures comes from conflicting results of theoretical studies.<sup>4,8–12</sup> MP2/6-31+G(d) calculations predict that the  $^2B_1$  and  $^2B_2$  states (with  $C_{2v}$  geometries) are nearly degenerate.<sup>12</sup> With a larger 6-311+G\* basis set, the  $C_{2v}$  ( $^2B_2$ ) isomer converts to a higher-symmetry  $D_{2h}$  ( $^2B_{3g}$ ) structure that lies 0.3 eV below the  $^2B_1$  state.<sup>11</sup> However, calculations with even larger basis sets support the earlier findings of the  $^2B_1$  state lying adiabatically below the  $^2B_2/{}^2B_{3g}$  state. The highest-level computational study to date<sup>8</sup> reports CCSD(T)/6-311+G(3df)

Received Date: June 20, 2010

Accepted Date: July 15, 2010

Published on Web Date: July 30, 2010

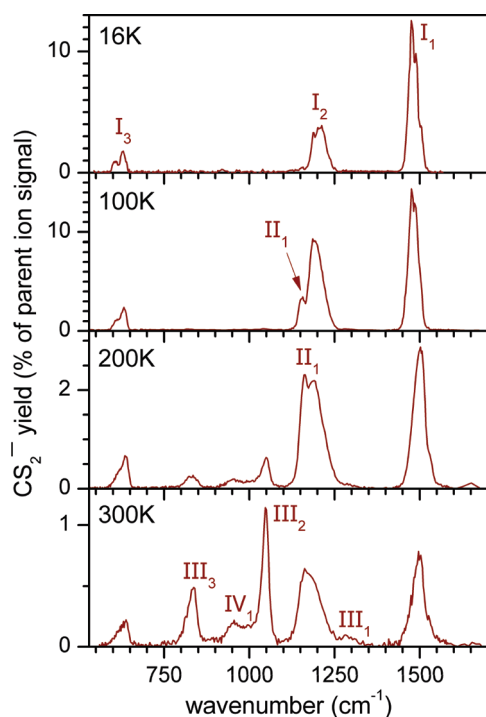


**Figure 1.** IRMPD spectra of mass-selected, buffer gas cooled  $(\text{CS}_2)_2^-$  ions recorded with trap temperatures of 16, 100, 200, and 300 K and monitoring the  $\text{CS}_2^-$  fragment ion peak. The spectra are normalized with respect to parent ion intensity. The features are labeled with Roman numerals I–IV, based on their appearance in the IRMPD spectra.

energies and predicts that the  $^2\text{B}_1$  state lies 0.11 eV below the  $^2\text{B}_2/{}^2\text{B}_{3g}$  state.

Herein, we present infrared multiple photon dissociation (IRMPD) spectra<sup>13,14</sup> of thermalized  $(\text{CS}_2)_2^-$  ions in the temperature range from 16 to 300 K. The IRMPD spectra were measured from 550 to 1750  $\text{cm}^{-1}$ , covering the region of the IR-active stretching vibrations of weakly and covalently bound  $(\text{CS}_2)_2^-$  isomers. The parent ion yield (prior to photodissociation) remains nearly constant over the complete temperature range. The only observed photofragment ion is  $\text{CS}_2^-$ . The spectra recorded with ion trap temperatures of 16, 100, 200, and 300 K are shown in Figure 1, and the bands are summarized in Table 1. In addition to the photofragments, we observed photoinduced electron emission below 200 K. The spectral features of the electron emission spectrum are comparable to those found when monitoring the  $\text{CS}_2^-$  fragment ion.

The IRMPD spectrum of  $(\text{CS}_2)_2^-$  measured at the lowest ion trap temperature studied (16 K) shows three main features labeled  $\text{I}_{1-3}$ . Each of these features exhibits vibrational substructure, suggesting the excitation of combinations bands involving a very low frequency mode ( $\sim 15 \text{ cm}^{-1}$ ). At 100 K, a new feature  $\text{II}_1$  appears slightly to the red ( $\sim 30 \text{ cm}^{-1}$ ) of the  $\text{I}_2$  band. At 200 K, feature  $\text{II}_1$  retains its approximate absolute intensity compared to the 100 K spectrum, while the I band's intensity decreases by roughly 80%. A set of four new features ( $\text{III}_{1-3}$  and  $\text{IV}_1$ ) are observed between 800 and 1350  $\text{cm}^{-1}$ . These features increase in relative intensity at 300 K, and  $\text{III}_2$  becomes the most intense peak. Unfortunately,

**Table 1.** Experimental IRMPD Band Positions  $\nu_{\text{exp}}$  (in  $\text{cm}^{-1}$ ) and Assignments Compared to the Calculated CCSD(T)/aug-cc-pVDZ and CCSD(T)/aug-cc-pVTZ Vibrational Frequencies  $\nu_{\text{harm}}$  (in  $\text{cm}^{-1}$ )<sup>a</sup>

band	$\nu_{\text{exp}}$	state	$\nu_{\text{harm}}^b$	mode
$\text{I}_1$	1475	$^2\text{A}'$	1486	$\text{CS}_2^-$ antisym. stretch
$\text{I}_2$	1212	$^2\text{A}'$	1169	$\text{CS}_2^-$ antisym. stretch
$\text{I}_3$	630	$^2\text{A}'$	628	sym. stretch out-of-phase
$\text{II}_1$	1157	$^2\text{A}_1$	1102 (1133)	antisym. stretch
$\text{III}_1$	1283	$^2\text{B}_1$	1366 (1362)	C–C stretch
$\text{III}_2$	1047	$^2\text{B}_1$	1058 (1069)	antisym. stretch out-of-phase
$\text{III}_3$	837	$^2\text{B}_1$	870 (878)	antisym. stretch in-phase
$\text{IV}_1$	955	$^2\text{B}_2$	985 (991)	antisym. stretch in-phase

<sup>a</sup> See Supporting Information for computational details. <sup>b</sup> CCSD(T)/aug-cc-pVTZ results are in parentheses.

the time required to change the trap temperature is much longer than the ion trapping time in the present experiment. We can therefore only study samples at a specific temperature, in contrast to running temperature cycles during a single trapping cycle. Summarizing, the IRMPD spectra in Figure 1 show evidence for at least three absorbing species I, II, and III, each with a unique IR signature and temperature dependence. For species I, bands  $\text{I}_1$  and  $\text{I}_2$  lie in between the frequencies of the antisymmetric stretch of  $\text{CS}_2$  (1530  $\text{cm}^{-1}$ )<sup>15</sup> and  $\text{CS}_2^-$  (1160  $\text{cm}^{-1}$ ),<sup>16</sup> making an assignment of I to the weakly bound  $\text{CS}_2 \cdot \text{CS}_2^-$  isomer reasonable. The previous IRPD spectrum of  $(\text{CS}_2)_3^-$ , which has a  $\text{CS}_2^-$  core solvated by two neutral  $\text{CS}_2$  molecules, showed vibrational frequencies of 1530 and 1215  $\text{cm}^{-1}$ ,<sup>5</sup> similar to  $\text{I}_1$  and  $\text{I}_2$ .

To aid our interpretation, we carried out electronic structure calculations using MOLPRO 06<sup>17</sup> and Gaussian 03<sup>18</sup> (see Supporting Information for details of the electronic structure methods employed in the present study). Optimized geometries and vibrational frequencies were determined up to the CCSD(T)/aug-cc-pVTZ level of theory. The CCSD(T)/aug-cc-pVTZ-optimized geometries along with the electronic state assignments and relative energies for the five lowest-energy  $(\text{CS}_2)_2^-$  isomers are shown in Figure 2. The complete list of optimized geometries is given in the Supporting Information. Also shown in Figure 2 are the simulated IR spectra for the different isomers derived from unscaled harmonic CCSD(T)/aug-cc-pVDZ frequencies and CCSD/aug-cc-pVDZ intensities.

In agreement with the previous CCSD(T) calculations,<sup>8</sup> we identify a four-membered ring  $C_{2v}$  symmetry structure ( $^2\text{B}_1$ ) as the ground state of  $(\text{CS}_2)_2^-$ . The  $^2\text{B}_2$  state is found to be 0.11 eV higher in energy (adiabatically). The previously reported  $D_{2h}$  and  $D_{2d}$  structures ( $^2\text{B}_{2g}$  and  $^2\text{A}_1$ , respectively) are 0.49 and 0.71 eV, respectively, above the  $^2\text{B}_1$  state.

The three absorption features of species I are satisfactorily reproduced by the simulated IR spectrum of the weakly bound ion–molecule complex of  $C_s$  symmetry (see Figure 3), supporting our assignment of these bands. In addition, this isomer exhibits a low-frequency in-plane librational mode (16  $\text{cm}^{-1}$ ) that can account for the observed vibrational substructure. Species II is characterized by a single, strong absorption band  $\text{II}_1$ , suggesting a structure of higher symmetry. Comparing the  $\text{II}_1$  position to theoretical results, the  $D_{2d}$  isomer gives the best agreement. This isomer is predicted to be nearly isoenergetic

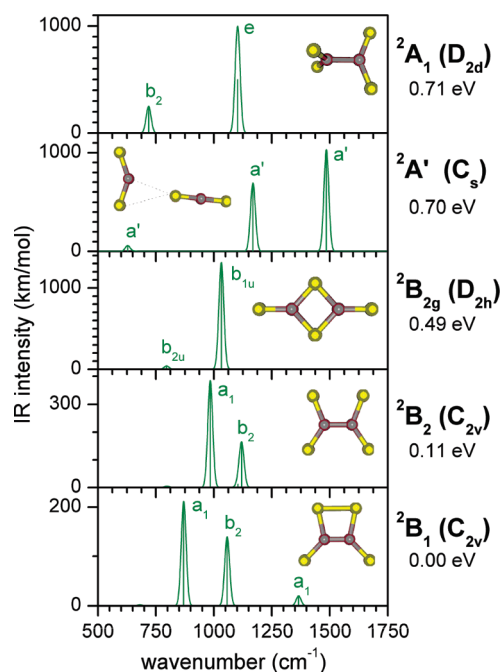


**Figure 2.** Optimized geometries, energies, and simulated linear absorption IR spectra of the five lowest-energy isomers of  $(\text{CS}_2)_2^-$ , corresponding to the (from top to bottom)  $^2A_1$ ,  $^2A'$ ,  $^2B_{2g}$ ,  $^2B_2$ , and  $^2B_1$  states. The CCSD(T)/aug-cc-pVTZ energies were calculated at the respective optimized geometries. The simulated spectra are derived from (unscaled) CCSD(T)/aug-cc-pVDZ harmonic frequencies and CCSD/aug-cc-pVDZ intensities, convoluted by a Gaussian line function with a fwhm width of 25  $\text{cm}^{-1}$ .

with the  $C_s$  structure and to exhibit its strongest absorption slightly below ( $-55 \text{ cm}^{-1}$ ) the  $\text{I}_2$  band, in reasonable agreement with the experimental observation ( $-30 \text{ cm}^{-1}$ ). In contrast to the  $C_s$  structure, in which the charge is localized predominantly on a bent  $\text{CS}_2^-$  core, in the  $D_{2d}$  isomer, the charge is equally shared between the two  $\text{CS}_2$  moieties.

The low absolute signal intensity associated with species III (note the different vertical scales for the 16 and 300 K spectra in Figure 1) implies that this species exhibits a smaller absorption cross section, less efficient internal vibrational energy redistribution, and/or requires more photons for dissociation, the latter suggesting a more strongly bound isomer. Of the three candidates,  $C_{2v}(^2B_1)$ ,  $C_{2v}(^2B_2)$ , and  $D_{2h}(^2B_{2g})$ , only the first yields a simulated IR spectrum that closely matches the positions of the three absorption bands  $\text{III}_{1-3}$  (see Figures 1–3). The dissociation energy of the  $C_{2v}(^2B_1)$  isomer, 0.95 eV,<sup>10</sup> is roughly five times larger than that of the  $C_s$  isomer ( $^2A'$ ). In combination with the smaller IR intensities predicted for the  $C_{2v}(^2B_1)$  structure (see Figure 2), this satisfactorily accounts for the lower absolute signal intensity of the III bands. The relative intensities of peaks  $\text{III}_2$  and  $\text{III}_3$  are reversed in the simulated spectrum for the  $C_{2v}(^2B_1)$  isomer (Figure 3) and may be attributed to the multiple photon absorption mechanism.<sup>13</sup>

Previous studies also found evidence for the  $C_{2v}(^2B_2)$  isomer in the anion photoelectron spectra.<sup>8</sup> In the present work, we observe a weak but distinct absorption feature at 951  $\text{cm}^{-1}$  ( $\text{IV}_1$ ) in the IRMPD spectra at 200 and 300 K. Band

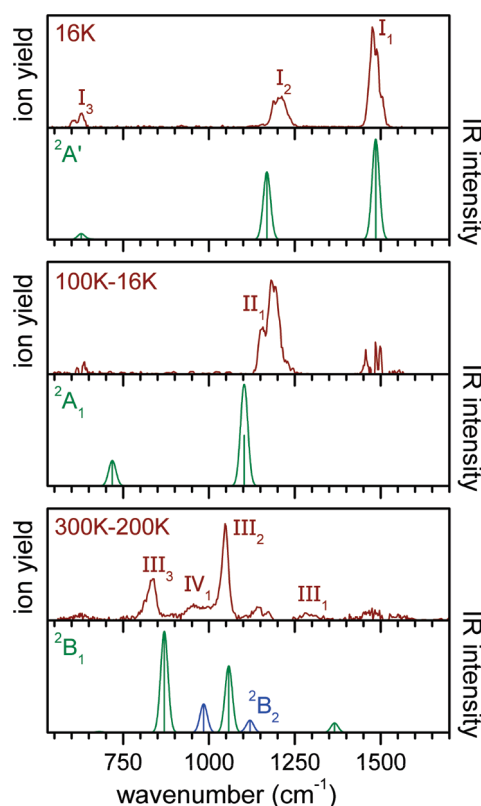


**Figure 3.** Experimental IRMPD difference spectra of  $(\text{CS}_2)_2^-$  ions obtained by scaling and subtracting the corresponding IRMPD spectra shown in Figure 1. The difference spectra are compared to simulated linear absorption IR spectra of the  $^2A'$ ,  $^2A_1$ ,  $^2B_1$ , and  $^2B_2$  states from Figure 2.

$\text{IV}_1$  cannot be assigned to a fundamental transition of species I, II, or III. We tentatively assign it to the most intense IR-active mode of the  $C_{2v}(^2B_2)$  isomer, whose spectrum is shown by the blue trace in Figure 3.

In summary, the three main absorbing species I, II, and III are assigned to the  $C_s(^2A')$ ,  $D_{2d}(^2A_1)$ , and  $C_{2v}(^2B_1)$  isomers of  $(\text{CS}_2)_2^-$ . This suggests the isomerization mechanism shown in Figure 4. Consistent with previous studies, the weakly bound  $\text{CS}_2 \cdot \text{CS}_2^-$  complex is mainly produced in the supersonic expansion and injected into the ion trap. At the low ion trap temperatures (16 K), this complex (I) is stable and predominantly present. The  $C_s$  potential minimum is separated from the nearly isoenergetic  $D_{2d}$  state by a small barrier. At temperatures of 100 K, sufficient internal energy ( $\geq 0.1 \text{ eV}$ ) is present to overcome this barrier. During the 199 ms trapping period, the ions equilibrate and efficiently transfer population from the initial  $C_s$  isomer to the  $D_{2d}$  isomer (II). Heating above 100 K gives access to isomer III (and IV) via internal conversion.<sup>12</sup> Subsequent collisions remove excess energy, leaving a covalently bound anion which cannot convert back to II (or I). The loss of I and II isomers to III is reflected in the temperature-dependent IR spectra by a corresponding decrease in the relative signal intensity.

The present results demonstrate how vibrational spectroscopy can be used to track a thermally induced intramolecular reaction from the entrance channel complex to

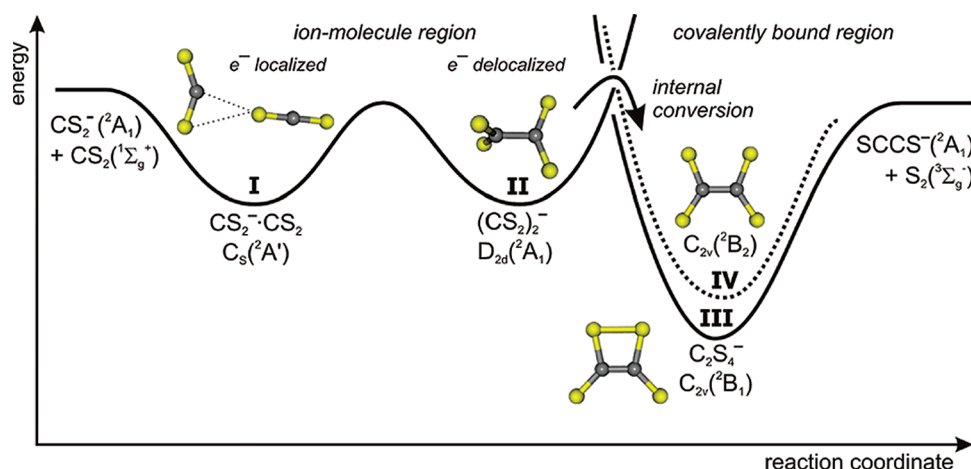


**Figure 4.** Proposed mechanism for isomer conversion of  $(\text{CS}_2)_2^-$  anions (see text). Species I ( $^2\text{A}'$ ) is mainly produced in the supersonic expansion and accumulated in the ion trap. At 16 K, the internal energy of species I is too small to overcome the isomerization barrier leading to species II ( $^2\text{A}_1$ ). At 100 K, species I and II are in equilibrium. At 200 K, species II is transformed via internal conversion to species III ( $^2\text{B}_1$ ) and IV ( $^2\text{B}_2$ ).

a covalently bound product in order to ultimately gain a better understanding of the influence of long-range dispersion forces on molecular reactions dynamics.<sup>19–21</sup> The  $(\text{CS}_2)_2^-$  system is particularly intriguing in that the barrier toward isomerization lies below the energy of the reactants, and thus, it represents an interesting model system for time-resolved studies aimed at unraveling the dynamics of internal conversion.

## EXPERIMENTAL SECTION

The IRMPD experiments are carried out using an ion trap/tandem mass spectrometer,<sup>22,23</sup> temporarily installed at the Free Electron Laser for Infrared eXperiments (FELIX) facility<sup>24</sup> at the FOM Institute Rijnhuizen (The Netherlands).  $(\text{CS}_2)_2^-$  anions are formed by secondary electron attachment in a supersonic expansion of  $\text{CS}_2$  vapor with Ar carrier gas at a backing pressure of  $\sim 8$  bar, which is crossed with high-energy electrons (1 keV). Anions are mass-selected by a quadrupole mass filter, deflected by  $90^\circ$ , and focused into a ring electrode ion trap filled with He buffer gas held at constant temperatures of 16, 100, 200, or 300 K. Collisions with He atoms thermalize the anions, which are accumulated in the trap for 199 ms and then extracted into the time-of-flight (TOF) mass spectrometer, where they interact with FELIX radiation prior to application of high-voltage pulses on the TOF electrodes. A mass spectrum is measured for each laser shot. IR spectra are recorded by scanning the laser wavelength and summing 15–25 mass spectra for each wavelength step. Fragment yields are reported as fractional intensities relative to the parent ion signal. The laser is operated from 500 to  $1750\text{ cm}^{-1}$  with a bandwidth of 0.25 % rms of the central wavelength and average power of  $\sim 15\text{ mJ/pulse}$ .

**SUPPORTING INFORMATION AVAILABLE** Theoretical methods, absolute and relative CCSD and CCSD(T) energies (Table S1), vibrational frequencies and intensities (Table S2), and optimized geometries (Table S3), as well as complete refs 17 and 18.

This material is available free of charge via the Internet at <http://pubs.acs.org>.

## AUTHOR INFORMATION

### Corresponding Author:

\*To whom correspondence should be addressed. E-mail: [sanov@u.arizona.edu](mailto:sanov@u.arizona.edu) (A.S.); [asmis@fhi-berlin.mpg.de](mailto:asmis@fhi-berlin.mpg.de) (K.R.A.).

**ACKNOWLEDGMENT** We would like to thank the Stichting voor Fundamenteel Onderzoek der Materie (FOM) for beam time and the staff for support and assistance. This research is funded by the European Community's Seventh Framework Programme (FP7/2007–2013), Grant n.°226716, and the U.S. National Science Foundation, Grant No. (CHE-0713880). L.J. thanks the Alexander von Humboldt Foundation for a postdoctoral scholarship. We thank Prof. M. Duncan for helpful comments.

## REFERENCES

- (1) Deluca, M. J.; Niu, B.; Johnson, M. A. Photoelectron-Spectroscopy of  $(\text{CO}_2)_n^-$  Clusters with  $2 \leq n \leq 13$ : Cluster Size Dependence of the Core Molecular Ion. *J. Chem. Phys.* **1988**, *88*, 5857–5863.
- (2) Shin, J.-W.; Hammer, N. I.; Johnson, M. A.; Schneider, H.; Glo, A.; Weber, J. M. An Infrared Investigation of the  $(\text{CO}_2)_n^-$  Clusters: Core Ion Switching from Both the Ion and Solvent Perspectives. *J. Phys. Chem. A* **2005**, *109*, 3146–3152.
- (3) Tsukuda, T.; Hirose, T.; Nagata, T. Negative-Ion Photoelectron Spectroscopy of  $(\text{CS}_2)_n^-$ : Coexistence of Electronic Isomers. *Chem. Phys. Lett.* **1997**, *279*, 179–184.
- (4) Maeyama, T.; Oikawa, T.; Tsumura, T.; Mikami, N. Photodestruction Spectroscopy of Carbon Disulfide Cluster Anions  $(\text{CS}_2)_n^-$ ,  $n = 1–4$ : Evidence for the Dimer Core Structure and Competitive Reactions of the Dimer Anion. *J. Chem. Phys.* **1998**, *108*, 1368–1376.
- (5) Kobayashi, Y.; Inokuchi, Y.; Ebata, T. Ion Core Structure in  $(\text{CS}_2)_n^+$  and  $(\text{CS}_2)_n^-$  ( $n = 3–10$ ) Studied by Infrared Photodissociation Spectroscopy. *J. Chem. Phys.* **2008**, *128*, 164319.
- (6) Bowen, K. H.; Eaton, J. G. Photodetachment Spectroscopy of Negative Cluster Ions. In *The Structure of Small Molecules and*



- Ions; Naaman, R., Vager, Z., Eds.; Plenum: New York, 1988; pp 147–169.
- (7) Habteyes, T.; Velarde, L.; Sanov, A. Effects of Isomer Coexistence and Solvent-Induced Core Switching in the Photodissociation of Bare and Solvated  $(\text{CS}_2)_2^-$  Anions. *J. Chem. Phys.* **2009**, *130*, 124301.
  - (8) Habteyes, T.; Velarde, L.; Sanov, A. Relaxation of  $(\text{CS}_2)_2^-$  to Its Global Minimum Mediated by Water Molecules: Photoelectron Imaging Study. *J. Phys. Chem. A* **2008**, *112*, 10134–10140.
  - (9) Matsuyama, Y.; Nagata, T. Structures of  $\text{C}_2\text{S}_4^-$  Molecular Anion: Photoelectron Spectroscopy and Theoretical Calculations. *Chem. Phys. Lett.* **2008**, *457*, 31–35.
  - (10) Hiraoka, K.; Fujimaki, S.; Aruga, K. Frontier-Controlled Structures of the Gas-Phase  $\text{A}^*(\text{CS}_2)$  Clusters,  $\text{A}^* = \text{S}_2^+$ ,  $\text{CS}_2^+$ ,  $\text{S}_2^-$ , and  $\text{CS}_2^-$ . *J. Phys. Chem.* **1994**, *98*, 1802–1809.
  - (11) Yu, L.; Zeng, A.; Xu, Q.; Zhou, M. Infrared Spectra of  $(\text{CS}_2)_2^-$  Anion in Solid Neon and Argon. *J. Phys. Chem. A* **2004**, *108*, 8264–8268.
  - (12) Sanov, A.; Lineberger, W. C.; Jordan, K. D. Electronic Structure of  $(\text{CS}_2)_2^-$ . *J. Phys. Chem. A* **1998**, *102*, 2509–2511.
  - (13) Oomens, J.; Sartakov, B. G.; Meijer, G.; von Helden, G. Gas-Phase Infrared Multiple Photon Dissociation Spectroscopy of Mass-Selected Molecular Ions. *Int. J. Mass Spectrom.* **2006**, *254*, 1–19.
  - (14) Asmis, K. R.; Fielicke, A.; von Helden, G.; Meijer, G. Vibrational Spectroscopy of Gas-Phase Clusters and Complexes. In *The Chemical Physics of Solid Surfaces. Atomic Clusters: From Gas Phase to Deposited*; Woodruff, D. P., Ed.; Elsevier: Amsterdam, The Netherlands, 2007; Vol. 12, pp 327–375.
  - (15) Wentink, T. Triatomic Linear Molecules Containing Carbon and Oxygen, Sulfur, Selenium, or Tellurium 0.1. Vibrational Spectra of  $\text{CS}_2$ ,  $\text{CSe}_2$ ,  $\text{SCSe}$ , and  $\text{SCTe}$ . *J. Chem. Phys.* **1958**, *29*, 188–200.
  - (16) Zhou, M. F.; Andrews, L. Infrared Spectra of the  $\text{CS}_2^-$ ,  $\text{CS}_2^+$ , and  $\text{C}_2\text{S}_4^+$  Molecular Ions in Solid Neon and Argon. *J. Chem. Phys.* **2000**, *112*, 6576–6582.
  - (17) Werner, H.-J.; Knowles, P. J.; Lindh, R.; Manby, F. R.; Schütz, M.; Celani, P.; Korona, T.; Rauhut, G.; Amos, R. D.; Bernhardsson, A.; et al. *MOLPRO*, version 2006.1, A Package of Ab Initio Programs; Turbomole GmbH: Karlsruhe, Germany, 2006.
  - (18) Frisch, M. J.; Trucks, G. W.; Schlegel, H. B.; Scuseria, G. E.; Robb, M. A.; Cheeseman, J. R.; Montgomery, J. J. A.; Vreven, T.; Kudin, K. N.; Burant, J. C.; et al. *Gaussian 03*, revision C.02; Gaussian, Inc.: Wallingford CT, 2004.
  - (19) Wheeler, M. D.; Anderson, D. T.; Lester, M. I. Probing Reactive Potential Energy Surfaces by Vibrational Activation of  $\text{H}_2$ –OH Entrance Channel Complexes. *Int. Rev. Phys. Chem.* **2000**, *19*, 501–529.
  - (20) Kupper, J.; Merritt, J. M. Spectroscopy of Free Radicals and Radical Containing Entrance-Channel Complexes in Superfluid Helium Nanodroplets. *Int. Rev. Phys. Chem.* **2007**, *26*, 249–287.
  - (21) Heaven, M. C. Spectroscopy and Dynamics of Hydride Radical van der Waals Complexes. *Int. Rev. Phys. Chem.* **2005**, *24*, 375–420.
  - (22) Goebbert, D. J.; Meijer, G.; Asmis, K. R. 10K Ring Electrode Trap-Tandem Mass Spectrometer for Infrared Spectroscopy of Mass Selected Ions. *AIP Conf. Proc.* **2009**, *1104*, 22–29.
  - (23) Goebbert, D. J.; Wende, T.; Bergmann, R.; Meijer, G.; Asmis, K. R. Messenger-Tagging Electrosprayed Ions: Vibrational Spectroscopy of Suberate Dianions. *J. Phys. Chem. A* **2009**, *113*, 5874–5880.
  - (24) Oepts, D.; van der Meer, A. F. G.; van Amersfoort, P. W. The Free-Electron-Laser User Facility Felix. *Infrared Phys. Technol.* **1995**, *36*, 297–308.